Journal of Scientific Computing, Vol. 16, No. 3, September 2001 (© 2001)

Some Aspects of the Method of Fundamental Solutions for Certain Harmonic Problems

Yiorgos-Sokratis Smyrlis[1] **and Andreas Karageorghis**[1]

Received May 16, 2001; accepted September 8, 2001

The Method of Fundamental Solutions (MFS) is a boundary-type method for the solution of certain elliptic boundary value problems. The basic ideas of the MFS were introduced by Kupradze and Alexidze and its modern form was proposed by Mathon and Johnston. In this work, we investigate certain aspects of a particular version of the MFS, also known as the Charge Simulation Method, when it is applied to the Dirichlet problem for Laplace's equation in a disk.

KEY WORDS: Method of fundamental solutions; circulant matrices; elliptic boundary value problems.

1. STATEMENT OF THE PROBLEM

We consider the boundary value problem

$$\begin{cases} \Delta u = 0 & \text{in } \Omega, \\ u = f & \text{on } \partial\Omega \end{cases} \tag{1.1}$$

where Δ denotes the Laplace operator and f is a given function. The domain Ω is the disk of radius ϱ,

$$\Omega = \{\mathbf{x} \in \mathbb{R}^2 : |\mathbf{x}| < \varrho\} \tag{1.2}$$

In the Method of Fundamental Solutions (MFS) (see [6, 19–21]), the solution u is approximated by

$$u_N(\mathbf{c}, \mathbf{Q}; P) = \sum_{j=1}^{N} c_j k(P, Q_j), \qquad P \in \bar{\Omega} \tag{1.3}$$

[1] Department of Mathematics and Statistics, University of Cyprus/*Πανεπιστήμιο Κύπρου*, P.O. Box 20537, 1678 Nicosia/*Λευκωσία*, Cyprus/*Κύπρος*. E-mail: andreask@ucy.ac.cy, smyrlis@ucy.ac.cy

0885-7474/01/0900-0341/0 © 2001 Plenum Publishing Corporation

where $\mathbf{c} = (c_1, c_2, \ldots, c_N)^T$ and $\mathbf{Q}$ is a $2N$-vector containing the coordinates of the singularities (sources) Q_j, $j = 1, \ldots, N$, which lie outside $\bar{\Omega}$. The function $k(P, Q)$ is a fundamental solution of Laplace's equation given by

$$k(P, Q) = -\frac{1}{2\pi} \log |P - Q| \tag{1.4}$$

with $|P - Q|$ denoting the distance between the points P and Q. The singularities Q_j are fixed on the boundary $\partial\tilde{\Omega}$ of a disk $\tilde{\Omega}$ concentric to Ω and defined by $\tilde{\Omega} = \{\mathbf{x} \in \mathbb{R}^2 : |\mathbf{x}| < R\}$, where $R > \varrho$. A set of collocation points $\{P_i\}_{i=1}^N$ is placed on $\partial\Omega$. If $P_i = (x_{P_i}, y_{P_i})$, then we take

$$x_{P_i} = \varrho \cos \frac{2(i-1)\pi}{N}, \qquad y_{P_i} = \varrho \sin \frac{2(i-1)\pi}{N}, \qquad i = 1, \ldots, N \tag{1.5}$$

If $Q_j = (x_{Q_j}, y_{Q_j})$, then

$$x_{Q_j} = R \cos \frac{2(j-1)\pi}{N}, \qquad y_{Q_j} = R \sin \frac{2(j-1)\pi}{N}, \qquad j = 1, \ldots, N \tag{1.6}$$

In the version of the MFS known as the Charge Simulation Method [8], the coefficients $\mathbf{c}$ are determined so that the boundary condition is satisfied at the boundary points $\{P_i\}_{i=1}^N$:

$$u_N(\mathbf{c}, \mathbf{Q}; P_i) = f(P_i), \qquad i = 1, \ldots, N \tag{1.7}$$

This yields a linear system of the form

$$G^0 \mathbf{c} = \mathbf{f} \tag{1.8}$$

for the coefficients $\mathbf{c}$, where the elements of the matrix G^0 are given by

$$G^0_{i,j} = -\frac{1}{2\pi} \log |P_i - Q_j|, \quad i, j = 1, \ldots, N \tag{1.9}$$

We are primarily interested in examining the behaviour of the approximation as the number of degrees of freedom N and the radius R of the exterior circle are varied. The global matrix G^0 has a special structure and its properties are given in Section 2.1.

In [7, 12, 15], it is shown that for analytic boundary data, the error in the MFS approximation satisfies

$$\sup_{P \in \Omega} |u(P) - u_N(P)| = O(\tau^N) \tag{1.10}$$

for a suitable $\tau < 1$; that is, exponential convergence is achieved. In the particular case where u is harmonic in the entire plane (see [12])

$$\sup_{P \in \Omega} |u(P) - u_N(P)| = O\left(\left(\frac{\varrho}{R}\right)^N\right) \tag{1.11}$$

If further we assume that the harmonic extension of u exists in the disk $\hat{\Omega} = \{\mathbf{x} \in \mathbb{R}^2 : |\mathbf{x}| < r_0\}$ where $R < r_0$, then it can be shown that [17]

$$\sup_{P \in \Omega} |u(P) - u_N(P)| \leqslant \frac{2}{1 - \frac{\varrho}{r_0}} \left((1 + C(R, \varrho)) \left(\frac{\varrho}{r_0}\right)^{\frac{N}{3}} + 4 \left(\frac{\varrho}{R}\right)^{\frac{N}{3}} \right) \cdot \sup_{|x| = r_0} |u(\mathbf{x})| \tag{1.12}$$

where

$$C(R, \varrho) = \max \left\{ 1, \left| \frac{\log(R^N + \varrho^N)}{\log(R^N - \varrho^N)} \right| \right\}$$

In [13, 14], these results is generalized to regions in the plane whose boundaries are analytic Jordan curves. In the recent work of [16], a practical rule is suggested for determining the collocation points and the singularities for any region using a suitable conformal mapping between an annulus-like neighborhood of the boundary and the standard annulus

$$A = \{\mathbf{x} \in \mathbb{R}^2 : \varrho < |\mathbf{x}| < R\}$$

Thus the collocation points and the singularities of this arbitrary region are the images, via this conformal mapping, of the uniformly distributed collocation points and corresponding singularities of the disk. In [17, 18], the stability of the MFS is examined in the case of the disk and it is observed that, although the method can be highly ill-conditioned, in the cases considered, this rarely affects the accuracy of the numerical solution [2].

In the above formulation there are two contradictory facts:

1. The MFS approximation (1.3) converges exponentially to the solution with N. (See (1.10)–(1.12).)

2. The condition number κ (in the 2-norm) of the matrix G^0, (1.9), grows exponentially with N. More precisely, it can be shown that [3, 17]

$$\kappa \sim \frac{\log R}{2} N \left(\frac{R}{\varrho}\right)^{\frac{N}{2}}$$

The poor conditioning of the MFS is widely reported in the literature (see e.g., [1, 2, 8, 17, 18]).

So far, the following question has not been satisfactorily addressed: *How does one select the parameters in the method (collocation points, singularities, fundamental solutions) in order to minimize the errors?*

In this work, we suggest some ways of addressing this question. The paper is organised as follows. In Section 2, we describe ways of reducing the error when the singularities are placed very close to the boundary or very far from it. We also describe an efficient way of implementing the method for the particular class of problems that we are studying, namely Dirichlet problems for Laplace's equation in a disk. In Section 3, we provide numerical evidence that these techniques improve the results. Finally, in Section 4, we give some concluding remarks and discuss other possibilities.

2. ROTATION AND NORMALIZATION

2.1. Rotation of the Singularities

In the case when the distance $\varepsilon = |R - \varrho|$ is very small, the matrix G^0 is well-conditioned as the values of its diagonal elements $G^0_{i,i}$, $i = 1, \ldots, N$, (which are all equal) become large and dominant as they behave like $O(\log \varepsilon)$. The behaviour of the conditioning of G^0, for different values of N, as ε varies can be seen from Fig. 1, where we calculated an estimate for the condition number κ_∞ of G_0 in the L_∞ norm using the NAG pair F07ADF-F07AGF [22]. Note that the peaks in the figure occur where the first eigenvalue vanishes and hence the condition number becomes infinite (see (2.12)). As observed in numerical experiments, as ε tends to zero, the numerical accuracy of the MFS deteriorates considerably. The reason for this is that in the MFS, we are essentially trying to approximate an integral of the form $\int_{\partial\Omega} \sigma(Q) \log r(P, Q)\, ds(Q)$ by a quadrature rule (see [8, Chapter 8]). As P approaches the boundary, the integrand becomes singular because of the logarithmic term and the quadrature rule becomes progressively less accurate. In this work, the collocation points $\{P_i\}_{i=1}^N$ are

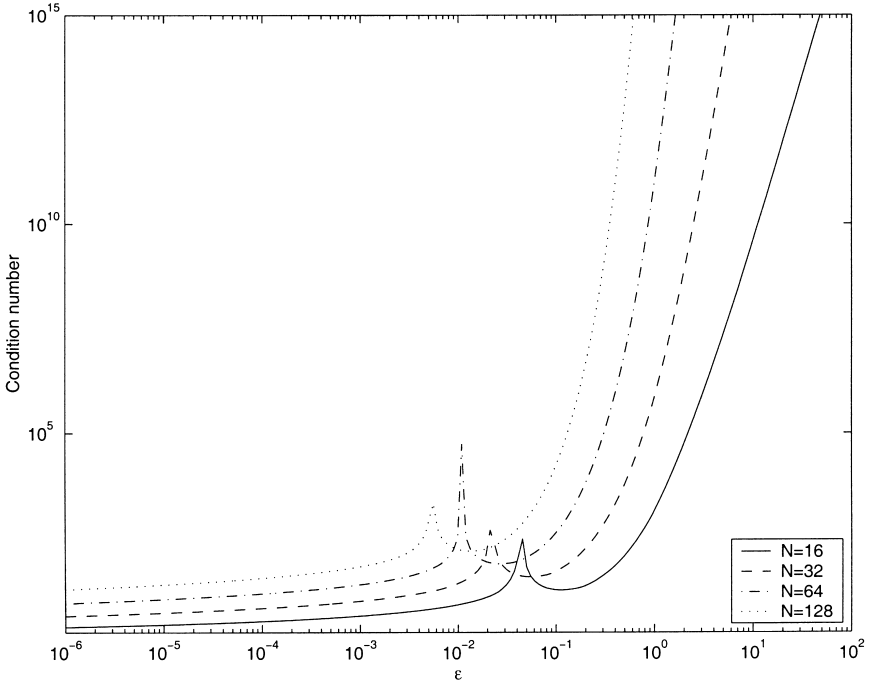

Fig. 1. Log–log plot of condition number versus ε for different N.

as in (1.5). The positions of the singularities are however *rotated*. The motivation for this approach is that once the singularities are rotated, the shortest distance from a singularity to a boundary point, becomes insensitive to ε (see (2.2)), as opposed to the case when the singularities are not rotated (see (2.3)). One advantage of this approach is that ε can even be taken equal to zero, i.e., the sources can be placed on the boundary. If we denote the coordinates of the singularity Q_j^α by $x_{Q_j^\alpha}$ and $y_{Q_j^\alpha}$, these become

$$x_{Q_j^\alpha} = R\cos\frac{2(j-1+\alpha)\,\pi}{N}, \quad y_{Q_j^\alpha} = R\sin\frac{2(j-1+\alpha)\,\pi}{N}, \qquad j=1,\ldots,N \tag{2.1}$$

where $0 \leqslant \alpha < 1$. This means that the positions of the sources differ by an angle $2\pi\alpha/N$ from the positions of the boundary points. Clearly, for every $i, j = 1,\ldots,N$

$$|P_i^\alpha - Q_j| \geqslant \varrho\,|e^{2\pi\alpha i/N} - 1|, \qquad \text{for} \quad \alpha \in (0,1) \tag{2.2}$$

whereas for every $i = 1,\ldots, N$

$$|P_i^0 - Q_i| = \varepsilon \tag{2.3}$$

The satisfaction of the boundary condition

$$u_N(\mathbf{c}, \mathbf{Q}^\alpha; P_i) = f(P_i), \qquad i = 1,\ldots, N$$

yields a linear system

$$G^\alpha \mathbf{c} = \mathbf{f}$$

with $\mathbf{c}$ the unknown vector, where the elements of the matrix G^α are

$$G^\alpha_{i,j} = -\frac{1}{2\pi} \log |P_i - Q_j^\alpha|, \qquad i, j = 1,\ldots, N \tag{2.4}$$

The matrix G^α, is insensitive to ε, for $\alpha \in (0, 1)$, in contrast to the matrix G^0, as is formally demonstrated by the following proposition.

Proposition. Let $G^\alpha = G^\alpha(\varepsilon)$ be the $N \times N$ matrix defined by (2.4) for $\alpha \in (0, 1)$ and $\varepsilon = |R - \varrho|$. Let ε_0 be a fixed positive number. Then there exists a positive constant M_0, depending on α, N and ε_0, such that

$$\|G^\alpha(\varepsilon)\| \leqslant M_0 \tag{2.5}$$

for every $\varepsilon \in [0, \varepsilon_0]$, whereas

$$\|G^0(\varepsilon)\| = O(\log \varepsilon) \tag{2.6}$$

where the matrix norm is defined by $\|G\| = \sup_{\|x\|_2 = 1} \|G\mathbf{x}\|_2$.

Proof. Without loss of generality, we assume that $\alpha \in (0, 1/2]$, because of the symmetry of the geometry about $\alpha = 1/2$. We observe that

$$\begin{aligned} |P_i - Q_j^\alpha|^2 &= (x_{P_i} - x_{Q_j^\alpha})^2 + (y_{P_i} - y_{Q_j^\alpha})^2 \\ &= (\varrho \cos \varphi_{i,0} - R \cos \varphi_{j,\alpha})^2 + (\varrho \sin \varphi_{i,0} - R \sin \varphi_{j,\alpha})^2 \end{aligned}$$

where $\varphi_{i,\alpha} = 2(i - 1 + \alpha)\, \pi/N$. Therefore

$$\left(\varrho - R \cos \frac{\alpha\pi}{N}\right)^2 + \left(R \sin \frac{\alpha\pi}{N}\right)^2 \leqslant |P_i - Q_j^\alpha|^2 \leqslant (R + \varrho)^2$$

and thus

$$\varrho \sin\frac{\alpha\pi}{N} \leqslant \varrho\left(\left(1-\cos\frac{\alpha\pi}{N}\right)^2+\left(\sin\frac{\alpha\pi}{N}\right)^2\right)^{1/2} \leqslant |P_i - Q_j^\alpha| \leqslant 2\varrho+\varepsilon_0$$

Therefore, if $G^\alpha = (G^\alpha_{i,j})_{i,j=1,\ldots,N}$ then

$$|G^\alpha_{i,j}| = \left|\log|P_i - Q_j^\alpha|\right| \leqslant \max\left\{\log\left(\varrho\sin\frac{\alpha\pi}{N}\right), \log(2\varrho+\varepsilon_0)\right\} = M_\alpha$$

Thus if $\mathbf{x} = (x_1,\ldots, x_N)$ then

$$\|G^\alpha\mathbf{x}\|_2^2 = \sum_{k=1}^N\left(\sum_{i=1}^N G^\alpha_{k,i}x_i\right)^2 \leqslant \sum_{k=1}^N\left(\sum_{i=1}^N (G^\alpha_{k,i})^2\right)\cdot\left(\sum_{i=1}^N x_i^2\right)$$
$$\leqslant N^2 \max_{k,i=1,\ldots,N}(G^\alpha_{k,i})^2\cdot\|\mathbf{x}\|_2^2$$

and finally,

$$\|G^\alpha\| \leqslant N\cdot M_\alpha$$

On the other hand, when $\alpha = 0$, we have that

$$-\frac{1}{2\pi}\log(R+\varrho) \leqslant G^0_{i,j} \leqslant -\frac{1}{2\pi}\log\varepsilon = G^0_{i,i}$$

Thus, as in the previous case

$$\|G^\alpha\mathbf{x}\|_2^2 \geqslant N^2 \max_{k,i=1,\ldots,N}(G^0_{k,i})^2\cdot\|\mathbf{x}\|_2^2$$

and

$$\|G^\alpha\| \leqslant N\frac{1}{2\pi}\log\left(\frac{1}{\varepsilon}\right)$$

whereas for $\mathbf{e} = (1, 0,\ldots, 0)$,

$$\|G^\alpha\mathbf{e}\| \geqslant |G^0_{1,1}| = \frac{1}{2\pi}\log\left(\frac{1}{\varepsilon}\right)$$

from which (2.6) follows. □

The basic properties of the matrix G^α are given in the following theorem:

Theorem. The matrix G^α has the following properties:

(i) The matrix G^α is circulant [4] for all $\alpha \in [0, 1)$.

(ii) When $N = 2m$, $m \in \mathbb{N}$, the matrix G^0 is symmetric of the form $circ(c_1, c_2, ..., c_m, c_{m+1}, c_m, ..., c_2)$.

(iii) When $N = 2m+1$, $m \in \mathbb{N}$ the matrix G^0 is symmetric of the form $circ(c_1, c_2, ..., c_m, c_m, c_{m-1}, ..., c_2)$.

(iv) When $N = 2m$, $m \in \mathbb{N}$, the matrix $G^{1/2}$ is singular (and non-symmetric) of the form $circ(c_1, c_2, ..., c_m, c_m, c_{m-1}, ..., c_1)$.

(v) When $N = 2m+1$, $m \in \mathbb{N}$ the matrix $G^{1/2}$ is non-singular (and non-symmetric) of the form $circ(c_1, c_2, ..., c_m, c_{m+1}, c_m, ..., c_1)$.

(vi) For $\alpha \neq 0, 1/2$ and any $N \in \mathbb{N}$ the matrix G^α is non-singular (and non-symmetric) of the form $circ(c_1, c_2, ..., c_N)$.

Proof. The matrix G^α is clearly circulant as each row is dependent on the distances of the boundary points from a fixed source. The next row is generated from the next source which is equivalent to rotating the circle (and boundary points) by an angle $2\pi/N$. Thus the first entry (distance) becomes the second one, the second entry becomes the third, and so on giving rise to a circulant matrix.

For (ii), the structure of the matrix is obvious from the symmetry of the geometry. To show that the matrix is symmetric, it is sufficient to observe that the entries $c_2, ..., c_m, c_{m+1}, c_m, ..., c_2$ in the first row of the matrix are symmetric about their middle element c_{m+1}.

Similarly, in (iii) to show that the matrix is symmetric, it is sufficient to observe that the entries $c_2, ..., c_m, c_m, c_{m-1}, ..., c_2$ are symmetric about their middle elements c_m, c_m.

In order to prove (iv), it is sufficient to observe that the sum of the m odd rows of the matrix $G^{1/2}$ is equal to the sum of the m even rows of $G^{1/2}$ which is equal to $\sum_{i=1}^{m} c_i$, thus the matrix $G^{1/2}$ is singular.

Results (v) and (vi) are trivial. □

We also prove the following properties of the matrix G^α.

Theorem. For $\varepsilon \ll 1$, the matrix $G^{1/6}$ has an eigenvalue $\lambda_1(1/6) = O(N\varepsilon)$. Otherwise, for general $\alpha \neq 0$, the corresponding eigenvalue of the matrix G^α is

$$\lambda_1(\alpha) = -\frac{1}{4\pi} \log(4 \sin^2(\pi\alpha)) + O(N\varepsilon)$$

In particular, when $\alpha = 0$, $\lambda_1(0) = O(\log(N\varepsilon))$.

Proof. In this and subsequent theorems, we shall assume, without loss of generality, that $\varrho = 1$.

We know that the matrix G^{α} is circulant. If $G^{\alpha} = circ(g_1(\alpha), g_2(\alpha),..., g_N(\alpha))$ the eigenvalues of G^{α} are given by

$$\lambda_j(\alpha) = \sum_{k=1}^{N} g_k(\alpha)\, \omega^{(j-1)(k-1)}, \qquad j = 1, 2,..., N \tag{2.7}$$

where $\omega = e^{\frac{2\pi i}{N}}$. Hence

$$\lambda_1(\alpha) = \sum_{k=1}^{N} g_k(\alpha) \tag{2.8}$$

But since

$$g_k(\alpha) = -\frac{1}{4\pi} \log\left((1+\varepsilon)^2 + 1 - 2(1+\varepsilon) \cos\left(\frac{2\pi(k+\alpha-1)}{N} \right) \right) \tag{2.9}$$

it follows that

$$\lambda_1(\alpha) = -\frac{1}{4\pi} \log \prod_{k=1}^{N} \left((1+\varepsilon)^2 + 1 - 2(1+\varepsilon) \cos\left(\frac{2\pi(k+\alpha-1)}{N} \right) \right)$$

or, from [9, p. 34]

$$\prod_{k=0}^{n-1} \left\{ x^2 - 2xy \cos\left(\alpha + \frac{2k\pi}{n} \right) + y^2 \right\} = x^{2n} - 2x^n y^n \cos n\alpha + y^{2n}$$

we have

$$\lambda_1(\alpha) = -\frac{1}{4\pi} \log((1+\varepsilon)^{2N} - 2(1+\varepsilon)^N \cos(2\pi\alpha) + 1) \tag{2.10}$$

Clearly, for $\alpha = 1/6$,

$$\lambda_1\left(\frac{1}{6}\right) = -\frac{1}{4\pi} \log(1 + (1+\varepsilon)^{2N} - 2(1+\varepsilon)^N)$$

$$= -\frac{1}{4\pi} \log(1 + O(N\varepsilon)) = O(N\varepsilon)$$

For general $\alpha \neq 0$,

$$\lambda_1(\alpha) = -\frac{1}{4\pi}\log(2(1+N\varepsilon)(1-\cos(2\pi\alpha))) + O(N\varepsilon) \tag{2.11}$$

which yields the result. Finally, for $\alpha = 0$,

$$\lambda_1(0) = -\frac{1}{2\pi}\log((1+\varepsilon)^N - 1) \tag{2.12}$$

thus

$$\lambda_1(0) = O(\log(N\varepsilon)) \qquad \square$$

Theorem. For $\varepsilon \ll 1$, the elements of the matrix G^α are given by

$$g_k(\alpha) = -\frac{1}{4\pi}\log\left(4\sin^2\left(\frac{\pi(k+\alpha-1)}{N}\right)\right) + O(\varepsilon), \qquad k = 1, 2, \ldots, N$$

Proof. From (2.9), ignoring terms of $O(\varepsilon^2)$, we obtain

$$g_k(\alpha) = -\frac{1}{4\pi}\log\left(2(1+\varepsilon)\left(1-\cos\left(\frac{2\pi(k+\alpha-1)}{N}\right)\right)\right) + O(\varepsilon^2)$$

$$= -\frac{1}{4\pi}\log\left(2\left(1-\cos\left(\frac{2\pi(k+\alpha-1)}{N}\right)\right)\right) + O(\varepsilon)$$

which yields the result. $\square$

The above two theorems lead to the following:

Corollary. For $\varepsilon = 0$, the elements of the matrix G^α are given by

$$g_k(\alpha) = -\frac{1}{4\pi}\log\left(4\sin^2\left(\frac{\pi(k+\alpha-1)}{N}\right)\right), \qquad k = 1, 2, \ldots, N$$

Also, the matrix $G^{1/6}$ is singular.

Proof. For the first part, we simply take $\varepsilon = 0$ in the expression for the elements of G^α in the general case when $\varepsilon \ll 1$.

For the second part, we observe that, when $\varepsilon = 0$, the eigenvalue $\lambda_1(1/6)$ is equal to zero. $\square$

We have examined the effect of rotating the singularities on the properties of the matrix G^α. The matrix remains circulant for all values of α. For certain angles α and small ε, however, the rotation gives rise to zero or very small eigenvalues. The significant improvement resulting from the application of this rotation technique, in particular when $\varepsilon \ll 1$, is demonstrated in Section 3 (see Fig. 4–7).

2.2. Normalization of the Fundamental Solutions

When ε is very large, the matrices G^α are badly conditioned, which could lead to poor results (see numerical results in Section 3.2). The poor conditioning of G^0 for large ε can be observed in Fig. 1. The conditioning of G^α is very similar for $\alpha \neq 0$.

In order to improve the accuracy of the numerical results for large ε, we also consider the normalized fundamental solution

$$\tilde{k}(P, Q) = -\frac{1}{2\pi} \log \frac{|P-Q|}{R}$$

instead of the fundamental solution (1.4). The idea of normalizing the fundamental solutions was introduced, in the MFS context, by Ho-Tai *et al.* [11] and also used by Han and Olson [10]. This modification leads to a normalized global matrix $\tilde{G}^\alpha$. From the definitions of G^0 and $\tilde{G}^0$, the elements of the two matrices satisfy (when $\varrho = 1$)

$$-\frac{1}{2\pi} \log(R+1) \leqslant G^0_{ij} \leqslant -\frac{1}{2\pi} \log(R-1), \qquad i, j = 1, 2, \ldots, N$$

and

$$-\frac{1}{2\pi} \log\left(1+\frac{1}{R}\right) \leqslant \tilde{G}^0_{ij} \leqslant -\frac{1}{2\pi} \log\left(1-\frac{1}{R}\right), \qquad i, j = 1, \ldots, N$$

This shows that as R grows, the elements of the unnormalized matrix G^0 grow much faster than the elements of $\tilde{G}^0$.

We next investigate the effect of this normalization on the condition number of the matrix of the system.

Proposition. For $\varepsilon \gg 1$, the eigenvalue $\lambda_1(0)$ of the matrix G^0 is $O(N \log R)$ whereas the corresponding eigenvalue $\tilde{\lambda}_1(0)$ of the matrix $\tilde{G}^0$ is $O(R^{-N})$. All the remaining eigenvalues of G^0 and $\tilde{G}^0$, are identical.

Proof. Since $\lambda_1(0) = \sum_{k=1}^{N} g_k(0)$ and

$$g_k(0) = -\frac{1}{4\pi} \log\left(R^2 + 1 - 2R\cos\left(\frac{2\pi(k-1)}{N}\right)\right)$$

it follows that

$$\lambda_1(0) = -\frac{1}{4\pi} \log \prod_{k=1}^{N} \left(R^2 + 1 - 2R\cos\left(\frac{2\pi(k-1)}{N}\right)\right)$$

or, from [9, p. 34],

$$\lambda_1(0) = -\frac{1}{4\pi} \log(R^{2N} - 2R^N + 1) = -\frac{1}{2\pi} \log(R^N - 1)$$

or

$$\lambda_1(0) = O(N \log R)$$

In the case of the normalized matrix $\tilde{G}^0$, we have

$$\tilde{g}_k(0) = -\frac{1}{4\pi} \log\left(R^{-2} + 1 - 2R^{-1}\cos\left(\frac{2\pi(k-1)}{N}\right)\right)$$

and therefore

$$\tilde{\lambda}_1(0) = -\frac{1}{4\pi} \log \prod_{k=1}^{N} \left(R^{-2} + 1 - 2R^{-1}\cos\left(\frac{2\pi(k-1)}{N}\right)\right)$$

or

$$\tilde{\lambda}_1(0) = -\frac{1}{4\pi} \log(R^{-2N} - 2R^{-N} + 1) = -\frac{1}{2\pi} \log(1 - R^{-N})$$

that is

$$\tilde{\lambda}_1(0) = O\left(\frac{1}{R^N}\right)$$

The other eigenvalues of G^0 are given by

$$\lambda_j(0) = \sum_{k=1}^{N} g_k(0)\, \omega^{(j-1)(k-1)}, \qquad j = 2, 3, \ldots, N \tag{2.13}$$

whereas the corresponding eigenvalues of $\tilde{G}^0$ are given by

$$\tilde{\lambda}_j(0) = \sum_{k=1}^{N} \tilde{g}_k(0)\, \omega^{(j-1)(k-1)}, \qquad j = 2, 3, \ldots, N$$

where $\tilde{g}_k(0) = g_k(0) - \frac{1}{2\pi} \log R$, $k = 1, 2, \ldots, N$. Thus for $j = 2, 3, \ldots, N$,

$$\begin{aligned} \tilde{\lambda}_j - \lambda_j &= \sum_{k=1}^{N} (\tilde{g}_k - g_k(0))\, \omega^{(j-1)(k-1)} \\ &= \sum_{k=1}^{N} \left(-\frac{1}{2\pi} \log R \right) \omega^{(j-1)(k-1)} \\ &= -\frac{1}{2\pi} \log R \sum_{k=1}^{N} \omega^{(j-1)(k-1)} = 0 \end{aligned}$$

hence

$$\tilde{\lambda}_j(0) = \lambda_j(0), \qquad j = 2, 3, \ldots, N \qquad \square$$

Proposition. For $\varepsilon \gg 1$, the condition number κ of the matrix G^0 is of $O(NR^{N/2} \log R)$ whereas the corresponding condition number of the matrix $\tilde{G}^0$ is of $O(NR^{N-1})$.

Proof. We first consider the case when N is even. From (2.13),

$$\lambda_j(0) = -\frac{1}{4\pi} \sum_{k=1}^{N} \log \left(1 - 2R \cos \left(\frac{2\pi(k-1)}{N} \right) + R^2 \right) e^{2\pi(j-1)(k-1)\, i/N}, \qquad j = 2, \ldots, N$$

By observing that in the series (2.14) the terms corresponding to $k = 1$ and $k = \frac{N}{2} + 1$ vanish, and that the pairs corresponding to $(k, N-k+2)$, $k = 2, \ldots, \frac{N}{2}$, cancel each other, we have that

$$\sum_{k=1}^{N} \log \left(1 - 2R \cos \left(\frac{2\pi(k-1)}{N} \right) + R^2 \right) \sin \left(\frac{2\pi(j-1)(k-1)}{N} \right) = 0 \qquad (2.14)$$

and therefore for $j = 2, \ldots, N$,

$$\lambda_j(0) = -\frac{1}{4\pi} \sum_{k=1}^{N} \log \left(1 - 2R \cos \left(\frac{2\pi(k-1)}{N} \right) + R^2 \right) \cos \left(\frac{2\pi(j-1)(k-1)}{N} \right) \qquad (2.15)$$

By also observing that,

$$\cos\left(\frac{2\pi(j-1)(k-1)}{N}\right)=\cos\left(\frac{2\pi(N-j+1)(k-1)}{N}\right),\qquad j=2,\ldots,\frac{N}{2}$$

it follows that

$$\lambda_j(0)=\lambda_{N-j+2}(0),\qquad j=2,\ldots,\frac{N}{2} \tag{2.16}$$

We wish to relate the above expressions for $\lambda_j(0)$, $j=2,\ldots,\frac{N}{2}$, to a definite integral for which we have an analytic expression. We therefore consider the integral

$$\int_0^{2\pi}\log(1-2R\cos\vartheta+R^2)\cos(j-1)\,\vartheta\,d\vartheta\,,\qquad j=2,3,\ldots,\frac{N}{2}$$

From [9, p. 593],

$$\int_0^{2\pi}\log(1-2a\cos\vartheta+a^2)\cos n\vartheta\,d\vartheta=-\frac{2\pi}{na^n}$$

we have for $j=2,3\ldots,N/2$, that

$$\int_0^{2\pi}\log(1-2R\cos\vartheta+R^2)\cos(j-1)\,\vartheta\,d\vartheta=-\frac{2\pi}{(j-1)\,R^{(j-1)}} \tag{2.17}$$

We now relate the above integral to the expression for $\lambda_j(0)$ via the composite trapezoidal rule. From this rule, it follows that

$$\begin{aligned}&\int_0^{2\pi}\log(1-2R\cos\vartheta+R^2)\cos(j-1)\,\vartheta\,d\vartheta\\&\quad=\int_0^{2\pi}f^j(\vartheta)\,d\vartheta\\&\quad=\frac{2\pi}{N}\left(\frac{1}{2}f^j_0+f^j_1+\ldots+f^j_{N-1}+\frac{1}{2}f^j_N\right)+E_N(f^j)\end{aligned} \tag{2.18}$$

where $f^j_k=\log(1-2R\cos\vartheta_k+R^2)\cos(j-1)\,\vartheta_k$, with $\vartheta_k=2\pi k/N$, $k=0,\ldots,N$. Since f^j is infinitely differentiable in ϑ and periodic (and therefore so are all its derivatives) it follows that for every $k\in\mathbb{N}$ there exists a $c_k>0$ such that $|E_N(f^j)|\leqslant c_k/N^{2k+1}$ for every $N\in\mathbb{N}$ (see [5]). (Numerically, we

have observed that E_N virtually vanishes for values of R larger than 2.) Since $f_0^j = f_N^j$, combining (2.17) and (2.18) we can write

$$\sum_{k=1}^{N} \log\left(1 - 2R\cos\left(\frac{2\pi(k-1)}{N}\right) + R^2\right)\cos\left(\frac{2\pi(j-1)(k-1)}{N}\right) \approx -\frac{N}{(j-1)\,R^{(j-1)}} \tag{2.19}$$

Therefore, combining (2.15), (2.16) and (2.19) we get

$$\lambda_j(0) \approx \frac{N}{4\pi(j-1)\,R^{(j-1)}}, \qquad j = 2, 3, \ldots, \frac{N}{2}$$

Similarly, it can be shown that $\lambda_{\frac{N}{2}+1}(0) \approx \frac{1}{\pi} R^{-\frac{N}{2}}$. This means that the largest of the eigenvalues $\lambda_j(0)$, $j = 1, 2, \ldots, N$, is $\lambda_1(0) = O(N \log R)$, and the smallest is $\lambda_{\frac{N}{2}+1}(0) = O(R^{-\frac{N}{2}})$. Hence the condition number of the the matrix G^0 is $O(NR^{\frac{N}{2}} \log R)$. For the matrix $\tilde{G}^0$, we have $\kappa(\tilde{G}^0) = O(NR^{N-1})$.

An identical argument reveals that in the case when N is odd, the eigenvalues satisfy

$$\lambda_j(0) = \lambda_{N-j+2}(0), \qquad j = 2, \ldots, \left[\frac{N}{2}\right] + 1$$

and hence the same result holds for the condition number. □

Despite the fact that the normalization does not improve the condition number, this does not seem to affect the numerical results (see Section 3). This is a consequence of the algorithm used for solving the system which does not involve standard Gaussian elimination methods for the solution of the system. This method of solution is described in the next section.

2.3. Numerical Implementation

In this section we describe the efficient implementation of the unnormalized method by exploiting the fact that the matrix to be inverted is circulant. Such matrices can be diagonalized efficiently by using Fast Fourier Transforms (FFT). We also describe how to avoid problems caused by zero or very small eigenvalues which appear for certain values of α and ε. The same analysis applies for the normalized method.

2.3.1. The Eigenvalues of the Matrix G^α

If the P_i's and Q_j's are points in the complex plane, the elements of G^α are

$$g_k(\alpha) = -\frac{1}{2\pi} \log |(1+\varepsilon)\, e^{\frac{2\pi\alpha i}{N}} - e^{\frac{2\pi(k-1)\, i}{N}}|, \qquad k = 1,\ldots, N$$

where $i = \sqrt{-1}$, When $\varepsilon = 0$, as the rotation parameter α approaches $1/6$, the first eigenvalue, $\lambda_1(\alpha)$ of G^α corresponding to the eigenvector $\xi_1 = \frac{1}{N^{1/2}}(1, 1,\ldots, 1)$, namely

$$\lambda_1(\alpha) = \sum_{k=1}^{N} g_k(\alpha) = -\frac{1}{2\pi} \log \left| \prod_{k=1}^{N} \left(e^{\frac{2\pi\alpha i}{N}} - e^{\frac{2\pi(k-1)\, i}{N}} \right) \right|$$

tends to zero. Specifically (see (2.10)) for δ small we have

$$\lambda_1(1/6+\delta) = -\frac{1}{4\pi} \log(2 - 2\cos(2\pi/6 + 2\pi\delta))$$

$$= -\frac{1}{4\pi} (2\pi\sqrt{3}\,\delta + O(\delta^2)) = -\frac{\sqrt{3}}{2}\delta + O(\delta^2)$$

whereas the other eigenvalues:

$$\lambda_m(\alpha) = \sum_{k=1}^{N} g_k(\alpha)\, \omega^{(k-1)(m-1)}, \qquad \omega = e^{2\pi i/N}, \qquad m = 2,\ldots, N$$

do not vanish for $\alpha \in [0, 1/2)$. The only other vanishing eigenvalue of G^α is $\lambda_{N/2+1}(\alpha)$ in the case N is even and $\alpha = 1/2$. Indeed, let $N = 2M$. Then

$$\lambda_{M+1}(1/2) = \sum_{k=1}^{N} g_k(1/2)\, \omega^{(k-1)\, M}$$

$$= \sum_{k=1}^{2M} \log |(1+\varepsilon)\, e^{\frac{\pi i}{2M}} - e^{\frac{\pi(k-1)\, i}{M}}|\, e^{(k-1)\, \pi i}$$

$$= \sum_{l=0}^{M-1} \log |(1+\varepsilon)\, e^{\frac{\pi i}{2M}} - e^{\frac{2l\pi i}{M}}| - \sum_{l=0}^{M-1} \log |(1+\varepsilon)\, e^{\frac{\pi i}{2M}} - e^{\frac{(2l+1)\, \pi i}{M}}|$$

$$= \sum_{l=0}^{M-1} \log |(1+\varepsilon) - e^{\frac{(4l-1)\, \pi i}{2M}}| - \sum_{l=0}^{M-1} \log |(1+\varepsilon) - e^{\frac{(4l+1)\, \pi i}{2M}}| = 0$$

A corresponding eigenvector is

$$\xi_{N/2+1} = \frac{1}{N^{1/2}}(-1, 1, -1, 1, \ldots, -1, 1)$$

The previous observations imply that the matrix G^α becomes extremely ill-conditioned, as α approaches $1/6$ and thus the computation of the approximate solution u_N is expected to generate large errors. Numerical experiments suggest, (see Section 3) that the approximation improves as $\alpha \to 1/6$, provided that the boundary data do not contain the eigenvector ξ_1, corresponding to the vanishing eigenvalue, or equivalently

$$\sum_{k=1}^{N} f(P_k) = 0$$

This fact is exploited in the design of our solution algorithm.

2.3.2. Inversion of the Circulant Matrix

For $\zeta = (\zeta_1, \ldots, \zeta_N)$, $\eta = (\eta_1, \ldots, \eta_N)$ vectors in $\mathbb{C}^N$, we define their complex inner product as $\langle \zeta, \eta \rangle = \sum_{k=1}^{N} \zeta_k \bar{\eta}_k$. By denoting the approximation $u_N(\mathbf{c}, \mathbf{Q}; P)$ in (1.3) by $u_N(P)$ we have

$$u_N(P) = \langle \mathbf{c}, \boldsymbol{l} \rangle = \langle (G^\alpha)^{-1} \mathbf{f}, \boldsymbol{l} \rangle = \langle \mathbf{f}, (G^\alpha)^{-*} \boldsymbol{l} \rangle \tag{2.20}$$

where $(G^\alpha)^{-*}$ is the conjugate transpose of the inverse of the circulant matrix G^α and

$$\boldsymbol{l} = \boldsymbol{l}(P) = -\frac{1}{2\pi}(\log|P - Q_1|, \ldots, \log|P - Q_N|)^T$$

We shall be using the following properties of circulant matrices: (see Davis [4]).

Properties. Let $A \in \mathbb{C}^{N \times N}$ be a circulant matrix, i.e., $A = \mathrm{circ}(a_1, \ldots, a_N)$. Then A is normal, i.e., $AA^* = A^*A$, and thus A is diagonalizable:

$$A = U^* D U \,, \qquad \text{where} \quad D = \mathrm{diag}(\mu_1, \ldots, \mu_N)$$

with eigenvalues

$$\mu_j = \sum_{k=1}^{N} a_k \omega^{(k-1)(j-1)}, \qquad \omega = e^{\frac{2\pi i}{N}}$$

and corresponding eigenvectors

$$\xi_j = \frac{1}{N^{1/2}}(1, \omega^{(j-1)}, \omega^{2(j-1)}, \ldots, \omega^{(n-1)(j-1)}), \qquad j = 1, \ldots, N$$

The vectors $\{\xi_1, \ldots, \xi_N\}$ form an orthonormal basis of $\mathbb{C}^N$. The matrix U is a unitary ($UU^* = I$) and its conjugate is the *Fourier matrix*

$$U^* = \frac{1}{N^{1/2}} \begin{pmatrix} 1 & 1 & 1 & \cdots & 1 \\ 1 & \omega & \omega^2 & \cdots & \omega^{N-1} \\ 1 & \omega^2 & \omega^4 & \cdots & \omega^{2(N-1)} \\ \vdots & \vdots & \vdots & & \vdots \\ 1 & \omega^{N-1} & \omega^{2(N-1)} & \cdots & \omega^{(N-1)(N-1)} \end{pmatrix}$$

In particular, if $\mathbf{v} \in \mathbb{C}^N$, then $\mathbf{v} = \sum_{k=1}^N \langle \mathbf{v}, \xi_k \rangle \xi_k$ and therefore

$$A\mathbf{v} = \sum_{k=1}^N \mu_k \langle \mathbf{v}, \xi_k \rangle \xi_k$$

Furthermore A^* is also circulant, and if A is nonsingular, its inverse is also circulant.

Since $\{\xi_k\}_{k=1,\ldots,N}$, form an orthonormal basis of $\mathbb{C}^N$, for nonsingular G^α we have

$$\begin{aligned}(G^\alpha)^{-*}\, \boldsymbol{l} &= (G^\alpha)^{-*} \sum_{k=1}^N \langle \boldsymbol{l}, \xi_k \rangle \xi_k \\ &= \sum_{k=1}^N \langle \boldsymbol{l}, \xi_k \rangle (G^\alpha)^{-*} \xi_k = \sum_{k=1}^N \bar{\lambda}_k^{-1}(\alpha) \langle \boldsymbol{l}, \xi_k \rangle \xi_k\end{aligned}$$

Thus (2.20) becomes

$$\begin{aligned}u_N(P) &= \langle \mathbf{f}, (G^\alpha)^{-*}\, \boldsymbol{l} \rangle \\ &= \sum_{k=1}^N \lambda_k^{-1}(\alpha) \langle \mathbf{f}, \xi_k \rangle \overline{\langle \boldsymbol{l}, \xi_k \rangle} \\ &= \lambda_1^{-1}(\alpha) \langle \mathbf{f}, \xi_1 \rangle \overline{\langle \boldsymbol{l}, \xi_1 \rangle} + \sum_{k=2}^N \lambda_k^{-1}(\alpha) \langle \mathbf{f}, \xi_k \rangle \overline{\langle \boldsymbol{l}, \xi_k \rangle} \end{aligned} \tag{2.21}$$

The sum $\sum_{k=2}^N \bar{\lambda}_k^{-1}(\alpha) \langle \boldsymbol{l}, \xi_k \rangle \xi_k$ remains bounded as $\alpha \to 1/6$, whereas $\lambda_1^{-1}(\alpha) \to -\infty$.

Remarks.

1. We thus have the following computational costs for the efficient evaluation of the following quantities, via FFT, for any $\alpha \in [0, 1/2]$ and $\varepsilon \geqslant 0$,

$$\begin{aligned} &\lambda_k(\alpha), && k = 1,\ldots, N \quad \text{Cost: } O(N \log N) \\ &\langle \mathbf{f}, \xi_k \rangle, && k = 1,\ldots, N \quad \text{Cost: } O(N \log N) \\ &\langle \boldsymbol{I}(P), \xi_k \rangle, && k = 1,\ldots, N \quad \text{Cost: } O(N \log N) \end{aligned}$$

   where P is an interior point of the unit circle. It should be noted that, in the case of approximating the solution at M interior points, the total computational cost is $O(MN \log N)$. The corresponding cost for the evaluation of the approximate solution at M interior points via Gaussian elimination is $O(N^3 + MN)$.
2. In MATLAB, the command for the solution of the linear system $A\mathbf{x} = \mathbf{b}$ where A is a nonsingular circulant matrix $A = circ(\mathbf{a})$, is particularly elegant: `x=fft(ifft(b)./fft(a))`

2.3.3. Description of the Algorithm

Numerical experiments with zero-average boundary conditions (i.e., $\sum_{k=1}^{N} f(P_k) = 0$), suggest that

$$\hat{u}_N(P) = \lim_{\alpha \to 1/6} \langle \mathbf{f}, (G^{\alpha})^{-*} \boldsymbol{I}(\alpha) \rangle \tag{2.22}$$

is the best approximation to the solution at P, when $\varepsilon = 0$. Unfortunately, this value cannot be obtained via the prescribed method of the rotated sources because the matrix $G^{1/6}$ is singular. The eigenvector corresponding to the vanishing eigenvalue $\lambda_1(1/6)$ is $\xi_1 = \frac{1}{N^{1/2}}(1, 1,\ldots, 1)$. If $\mathbf{f}$ does not contain ξ_1, i.e.

$$\langle \mathbf{f}, \xi_1 \rangle = \sum_{k=1}^{N} f(P_k) = 0$$

then (2.22) becomes

$$\begin{aligned} \hat{u}_N(P) &= \langle \mathbf{f}, U^* D^+ U \boldsymbol{I}(1/6) \rangle \\ &= \sum_{k=2}^{N} \lambda_k^{-1}(1/6) \langle \mathbf{f}, \xi_k \rangle \overline{\langle \boldsymbol{I}, \xi_k \rangle} \end{aligned}$$

by virtue of (2.21), where $D^+ = \text{diag}(0, \bar{\lambda}_2^{-1}(1/6),\ldots, \bar{\lambda}_N^{-1}(1/6))$. This observation leads to an efficient algorithm for computing the approximate solution:

For any interior point P in the unit circle, we have

$$u_N(P) = \langle (G^\alpha)^{-1}\mathbf{f}, \boldsymbol{l}\rangle = \sum_{k=1}^{N} \lambda_k^{-1}(\alpha)\langle \mathbf{f}, \xi_k\rangle\overline{\langle \boldsymbol{l}, \xi_k\rangle} \tag{2.23}$$

provided that none of the eigenvalues vanishes. When $\alpha = 1/6$ and $\varepsilon = 0$, as $\lambda_1(1/6) = 0$, the expression (2.23) is no longer applicable. However, if the average value of the vector $\mathbf{f}$ is zero, (i.e., $\frac{1}{N}\sum_{k=1}^{N} f(P_k) = 0$ and as a consequence $\langle \mathbf{f}, \xi_1\rangle = \frac{1}{N^{1/2}}\sum_{k=1}^{N} f(P_k) = 0$), then the first term in the sum (2.23) can be discarded. In the case when the average value of the vector $\mathbf{f}$ is non-zero, we can decompose $\mathbf{f}$ as

$$\mathbf{f} = \mathbf{f} - \langle \mathbf{f}, \xi_1\rangle \xi_1 + \langle \mathbf{f}, \xi_1\rangle \xi_1$$

The first part of the right hand side of the above decomposition, namely

$$\mathbf{f}^0 = \mathbf{f} - \langle \mathbf{f}, \xi_1\rangle \xi_1$$

has clearly zero average, while the remaining part

$$\mathbf{f}^1 = \langle \mathbf{f}, \xi_1\rangle \xi_1$$

is a constant multiple of ξ_1. From this decomposition we consider two harmonic Dirichlet boundary value problems, one with zero-average boundary data (corresponding to $\mathbf{f}^0$) and with approximate solution

$$u_N^0(P) = \sum_{k=2}^{N} \lambda_k^{-1}\left(\frac{1}{6}\right)\langle \mathbf{f}, \xi_k\rangle\overline{\langle \boldsymbol{l}, \xi_k\rangle} \tag{2.24}$$

and one with constant boundary data (corresponding to $\mathbf{f}^1$), and hence with constant (exact) solution

$$u_N^1(P) = \frac{1}{N^{1/2}}\langle \mathbf{f}, \xi_1\rangle$$

Since the problem is linear, our approximate solution is simply obtained by superposition

$$u_N(P) = u_N^0(P) + u_N^1(P)$$

Furthermore, it should be mentioned that in another case where a zero eigenvalue is encountered, namely when N is even and $\alpha = 1/2$, a similar analysis is applicable. In this case the eigenvalue $\lambda_{N/2+1}(1/2)$ vanishes and it has corresponding normalized eigenvector $\xi_{N/2+1} = \frac{1}{N^{1/2}}(-1, 1, -1, 1, \ldots, -1, 1)$. As before, we omit from the sum (2.23) the term corresponding to

$k = N/2+1$. (This amounts to subtracting $\langle \mathbf{f}, \xi_{N/2+1} \rangle \xi_{N/2+1}$ from $\mathbf{f}$.) After computing the approximate solution of the boundary value problem with boundary data $\mathbf{f} - \langle \mathbf{f}, \xi_{N/2+1} \rangle \xi_{N/2+1}$, which is

$$u_N^0(P) = \sum_{1 \leqslant k \leqslant N, k \neq N/2+1} \lambda_k^{-1} \left(\frac{1}{2}\right) \langle \mathbf{f}, \xi_k \rangle \overline{\langle \mathbf{l}, \xi_k \rangle}$$

we superpose to it the harmonic function

$$u_N^{N/2+1}(P) = \frac{1}{N^{1/2}} \langle \mathbf{f}, \xi_{N/2+1} \rangle \, \mathsf{Re}(z(P)^{N/2}) \tag{2.25}$$

where $z(P)$ is the representation of the point P in the complex plane (i.e., $z(P) = x_P + iy_P$) and Re denotes the real part of a complex number. The harmonic function in (2.25) agrees with the vector $\mathbf{f}^{N/2+1} = \langle \mathbf{f}, \xi_{N/2+1} \rangle \xi_{N/2+1}$, at the boundary nodes P_k, $k = 1,\ldots, N$, (i.e., the harmonic function $u_N^{N/2+1}$ at the boundary point P_k is equal to the kth component of $\mathbf{f}^{N/2+1}$). The solution in this case is therefore

$$u_N(P) = u_N^0(P) + u_N^{N/2+1}(P)$$

Summarizing, in the case when $\alpha = 1/6$ and $\varepsilon = 0$ we have the approximation

$$u_N(P) = \sum_{k=2}^{N} \lambda_k^{-1} \left(\frac{1}{6}\right) \langle \mathbf{f}, \xi_k \rangle \overline{\langle \mathbf{l}, \xi_k \rangle} + \frac{1}{N} \sum_{k=1}^{N} f(P_k)$$

whereas in the case when $\alpha = 1/2$ and $\varepsilon \geqslant 0$, we have (for N even)

$$u_N(P) = \sum_{1 \leqslant k \leqslant N, k \neq N/2+1} \lambda_k^{-1} \left(\frac{1}{2}\right) \langle \mathbf{f}, \xi_k \rangle \overline{\langle \mathbf{l}, \xi_k \rangle} + \left(\frac{1}{N} \sum_{k=1}^{N} (-1)^k f(P_k)\right) \mathsf{Re}(z(P)^{N/2})$$

Note. For implementational purposes, one could use the modified expression

$$u_N(P) = \sum_{2 \leqslant k \leqslant N, k \neq N/2+1} \lambda_k^{-1}(\alpha) \langle \mathbf{f}, \xi_k \rangle \overline{\langle \mathbf{l}, \xi_k \rangle} + \frac{1}{N} \sum_{k=1}^{N} f(P_k) + \left(\frac{1}{N} \sum_{k=1}^{N} (-1)^k f(P_k)\right) \mathsf{Re}(z(P)^{N/2}) \tag{2.26}$$

which accommodates all values of α and ε except for $\alpha = \varepsilon = 0$, including the cases of vanishing eigenvalues, $\alpha = 1/6$, $\varepsilon = 0$ and $\alpha = 1/2$, $\varepsilon \geqslant 0$.

Equation (2.26) describes a hybrid method in which the boundary data $\mathbf{f}$ is split into two parts, namely, a first part corresponding to the eigenvectors ξ_1 and $\xi_{N/2+1}$, and a second part corresponding to the remaining eigenvectors. For the second part, we use the method of solution given by (2.23) (clearly the terms coresponding to $k = 1$ and $k = N/2+1$ do not appear in the sum since their contribution to the boundary data has been removed). For the first part, we find two harmonic functions, namely the constant function and $\mathrm{Re}(z(P)^{N/2})$, such that a linear combination of these agrees with this (first) part at the boundary points.

The above analysis is valid for even values of N. When N is odd (2.26) is replaced by

$$u_N(P) = \sum_{k=2}^{N} \lambda_k^{-1}(\alpha) \langle \mathbf{f}, \xi_k \rangle \overline{\langle \mathbf{l}, \xi_k \rangle} + \frac{1}{N} \sum_{k=1}^{N} f(P_k)$$

3. NUMERICAL RESULTS

We considered two problems with $\varrho = 1$ and exact solutions $u = x^2 - y^2$ (Example 1) and $u = e^x \cos y$ (Example 2). We varied the radius R of the external circle and examined how this affected the accuracy of the solution and the conditioning of the matrix G^α for various values of N. The typical behaviour of the conditioning of G^α can be seen in Fig. 1 in the case $\alpha = 0$. The behaviour for $\alpha \neq 0$ is very similar. The calculated MFS solution was compared with the analytical solution of the problems and the error calculated on a grid of boundary points defined by $(x, y) = (\cos \vartheta_j, \sin \vartheta_j)$, $\vartheta_j = 2\pi j/1024$, $j = 0, 1, \ldots, 1023$. For each value of R, we calculated the largest relative error $E = \|u - u_N\|_\infty / \|u\|_\infty$ in the solution for the cases $N = 2^2, 2^3, \ldots, 2^{10}$. In Fig. 2, we plot the log of the maximum relative error E versus $\log R$ for $N = 2^4, 2^5, 2^6, 2^7$ for Example 1. It was observed that, close to the boundary (i.e., for values of $R \leqslant 1.1$) the maximum relative error behaves like $O(R^{-N})$. Subsequently, for values of $R \geqslant 10$, the maximum relative error deteriorates like $O(R^2)$. From the numerical results of Fig. 2, it appears that the MFS approximation is poor when the distance $\varepsilon = |R - \varrho|$ is either very small or very large. Similar conclusions can be drawn from Fig. 3, where we present the graph of the maximum relative error E versus $\log R$ for $N = 2^4, 2^5, 2^6, 2^7$, for Example 2.

3.1. Case $\varepsilon \ll 1$

In order to address the problems encountered when $\varepsilon \ll 1$ and $\alpha = 0$, we examined the case when $\alpha \neq 0$, in particular $0 < \alpha \leqslant 1/2$, because of the

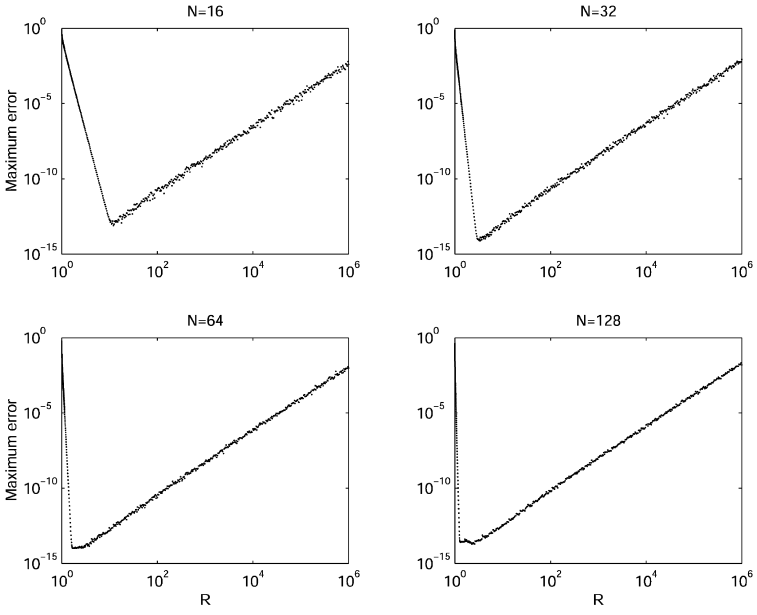

Fig. 2. Error versus the radius R for the function $u(x, y) = x^2 - y^2$.

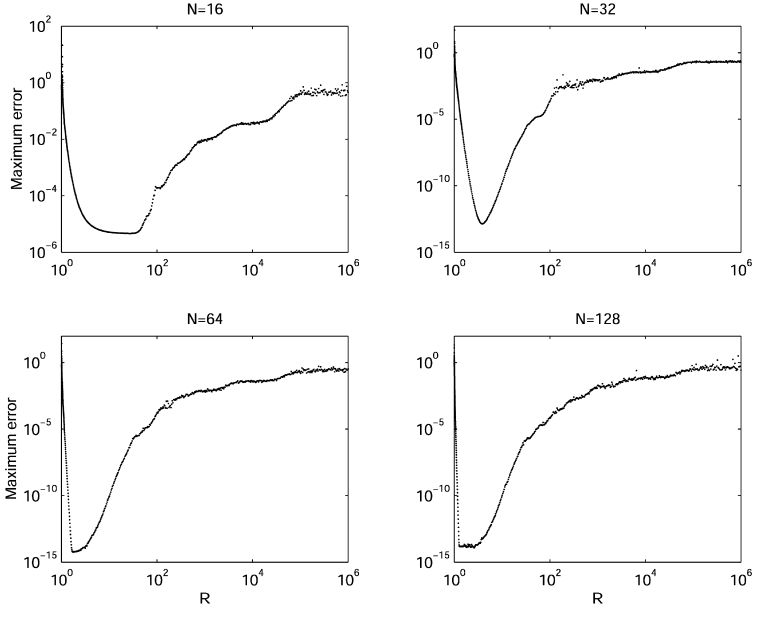

Fig. 3. Error versus the radius R for the function $u(x, y) = e^x \cos y$.

symmetry of the problem about $\alpha = 1/2$. For certain fixed values of ε, we calculated the maximum relative error for $N = 2^3, 2^4, 2^5, 2^6, 2^7$, for values of $\alpha \in (0, 1/2)$ for Examples 1 and 2. In Figs. 4–8, we present the log of the maximum relative error versus α in the cases $\varepsilon = 10^{-11}, 10^{-6}, 10^{-2}, 10^{-1}, 1$.

Our numerical results reveal that

1. If $2\pi/N \gg \varepsilon = R-1$, then the error is optimized when $\alpha = 1/6$.
2. If $2\pi/N \ll \varepsilon = R-1$, then the error is optimized when $\alpha = 1/4$.

3.2. Case $\varepsilon \gg 1$

In the case of large ε we studied the effect of normalizing the fundamental solutions as described in Section 2.2. The numerical results indicate that this normalization leads to improved accuracy in the MFS approximation. In Figs. 9–12, we present the log of the maximum relative error versus $\log R$ for normalized and unnormalized fundamental solutions, for $N = 2^4, 2^5, 2^6, 2^7$ for both examples. For small values of R, the behaviour of the errors is identical. For large values of R, however, there is improved accuracy for normalized fundamental solutions.

4. DISCUSSION AND EXTENSIONS

Some of the numerical difficulties associated with the application of the MFS to circular geometries, namely the poor accuracy of the method when the singularities are placed either very close to or very far from the boundary, have been investigated and ways of overcoming these suggested. In the case where the curve on which the sources are placed is located very close to the boundary, it appears that the angular positioning of these is of crucial importance. In the case where the artificial boundary is located very far from the boundary, a normalization of the fundamental solutions leads to improved accuracy. In an effort to overcome some of the conditioning problems associated with the MFS in the latter case, we also considered the solution of a linear least squares problem by taking M boundary points instead of N in Eq. (1.5), the number of sources remaining $N(< M)$. The resulting system of M linear equations in N unknowns was solved using the least-squares NAG routine F04ANF [22]. Despite extensive experimentation with M and N, we were unable to deduce that a larger number of M leads to improved accuracy for large R. We also examined the case of mixed boundary conditions, namely the case when we have Dirichlet conditions on part of the boundary and Neumann on the remaining part. Preliminary results indicate that the behaviour of the error and the condition number are similar to the case of Dirichlet boundary conditions.

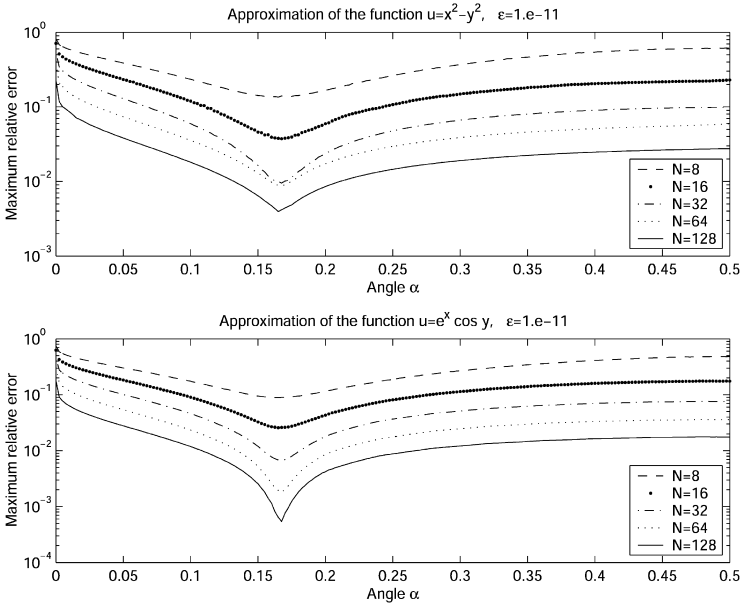

Fig. 4. Approximation error of rotated sources when $\varepsilon = R - 1 = 10^{-11}$.

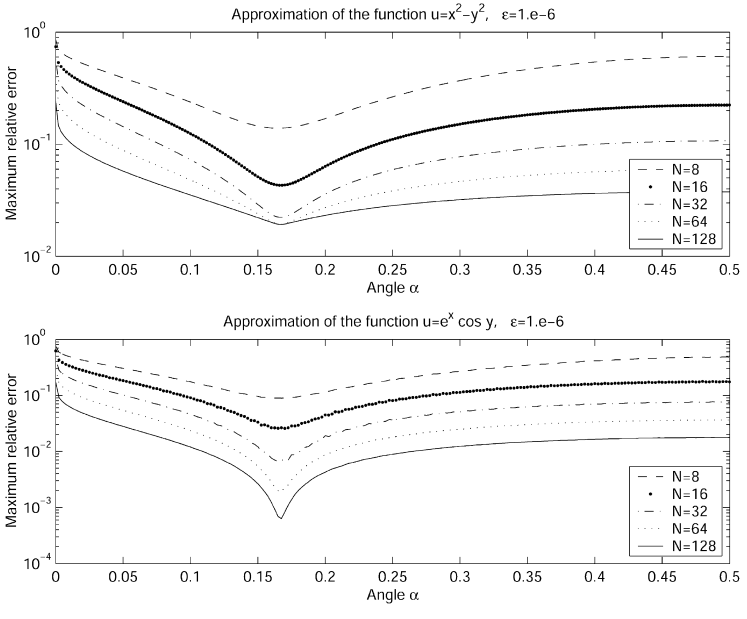

Fig. 5. Approximation error of rotated sources when $\varepsilon = R - 1 = 10^{-6}$.

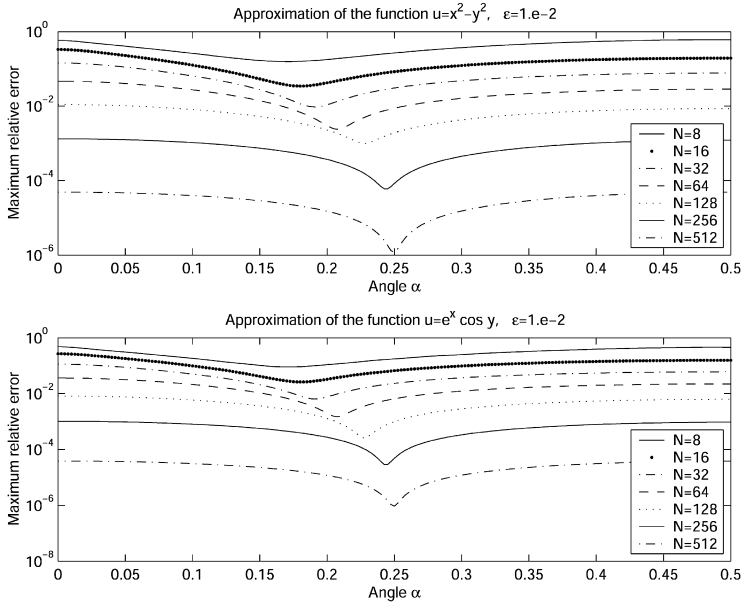

Fig. 6. Approximation error of rotated sources when $\varepsilon = R - 1 = 10^{-2}$.

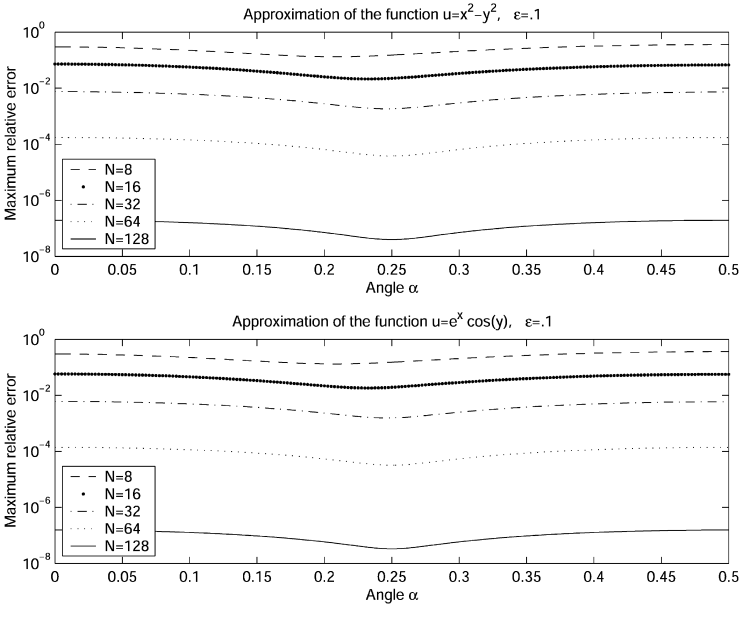

Fig. 7. Approximation error of rotated sources when $\varepsilon = R - 1 = 10^{-1}$.

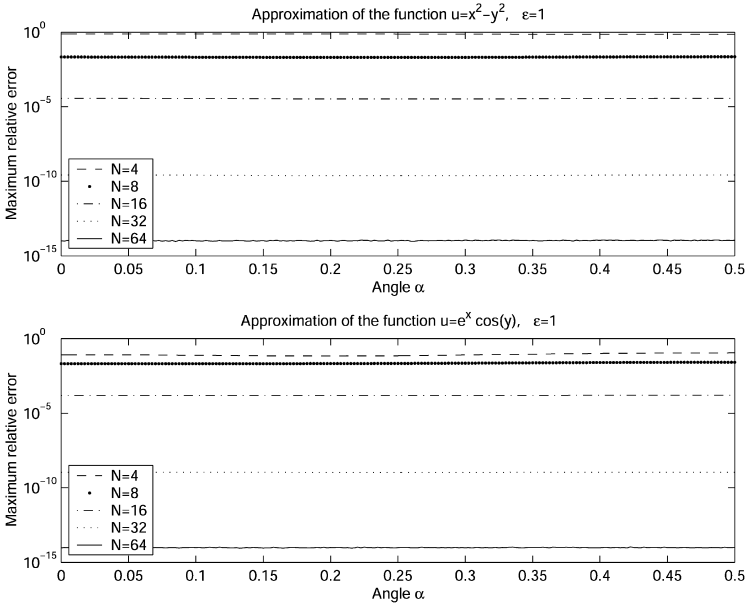

Fig. 8. Approximation error of rotated sources when $\varepsilon = R - 1 = 1$.

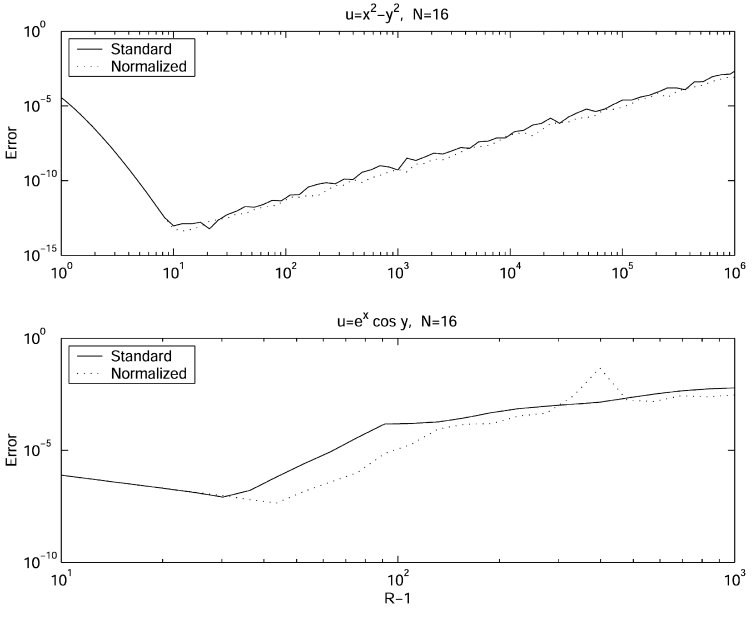

Fig. 9. Approximation with *unnormalized* versus *normalized* fundamental solutions.

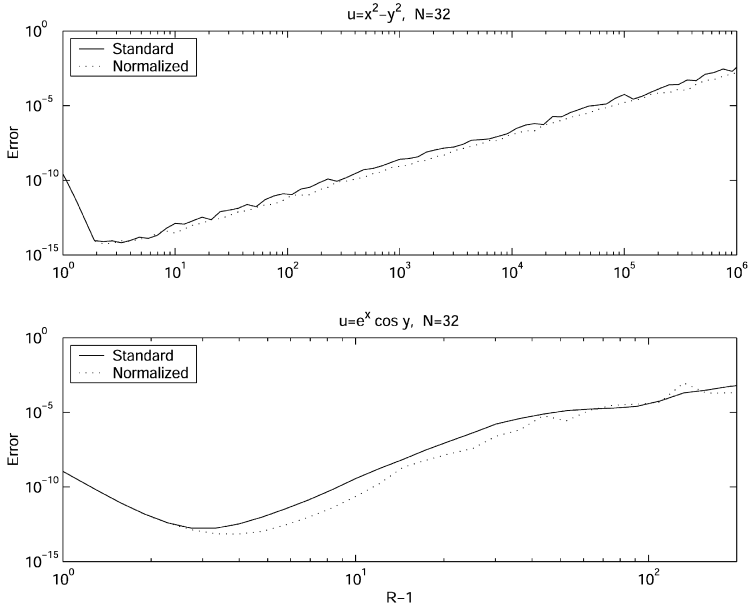

Fig. 10. Approximation with *unnormalized* versus *normalized* fundamental solutions.

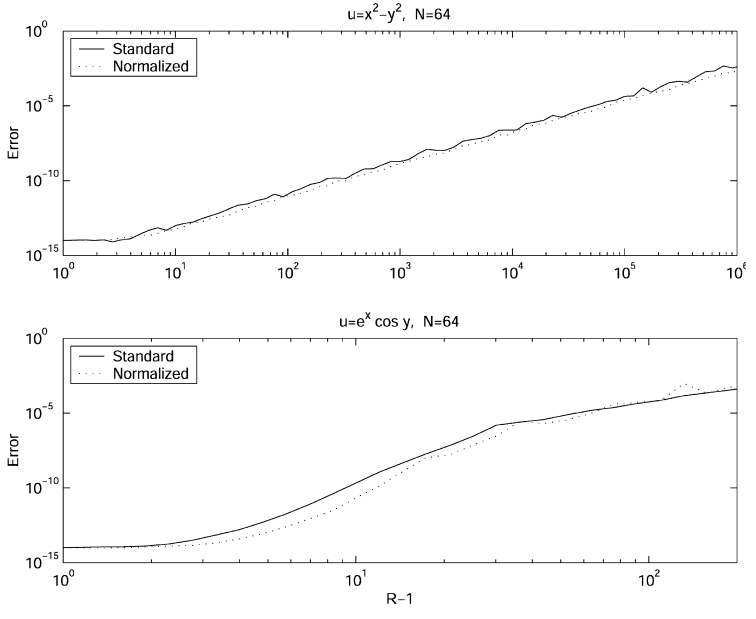

Fig. 11. Approximation with *unnormalized* versus *normalized* fundamental solutions.

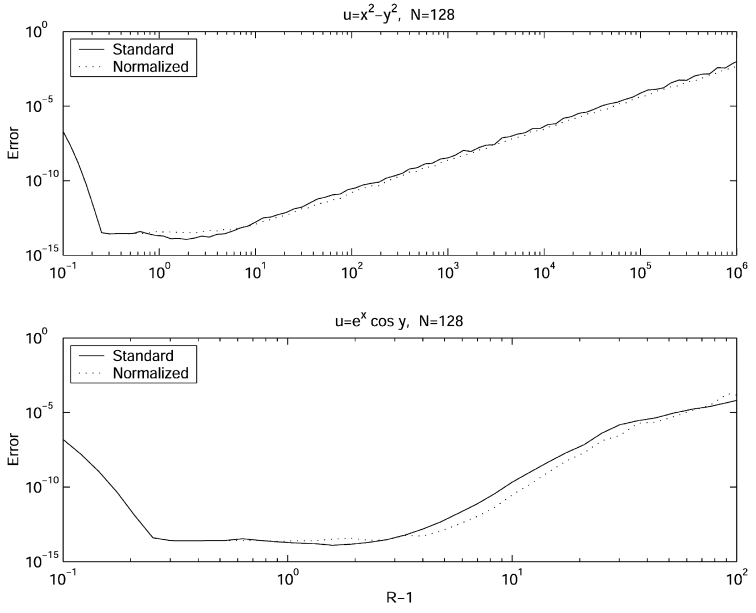

Fig. 12. Approximation with *unnormalized* versus *normalized* fundamental solutions.

We also experimented with the boundary value problem (1.1) on the ellipse

$$\Omega = \left\{ \mathbf{x} \in \mathbb{R}^2 : \frac{x^2}{a^2} + \frac{y^2}{b^2} < 1 \right\}$$

which is the ellipse with major axis $2a$ and minor axis $2b$, with the singularities being placed on the boundary of the ellipse

$$\tilde{\Omega} = \left\{ \mathbf{x} \in \mathbb{R}^2 : \frac{x^2}{R_a^2} + \frac{y^2}{R_b^2} < 1 \right\}$$

The coordinates of the boundary point P_i are

$$x_{P_i} = a \cos \frac{2(i-1)\,\pi}{N}, \qquad y_{P_i} = b \sin \frac{2(i-1)\,\pi}{N}, \qquad i = 1, 2, \ldots, N$$

and the coordinates of the singularity Q_j

$$x_{Q_j} = R_a \cos \frac{2(j-1+\alpha)\,\pi}{N}, \quad y_{Q_j} = R_b \sin \frac{2(j-1+\alpha)\,\pi}{N}, \qquad j = 1, 2, \ldots, N \tag{4.2}$$

where $0 \leqslant \alpha < 1$ and $R_b = \frac{b}{a} R_a$. In this case, the global matrix is no longer circulant. The method was tested on the two problems with $b = 1$ and exact solutions $u = x^2 - y^2$ and $u = e^x \cos y$, in the two cases $a = 1/2$ and $a = 1/4$. It was observed that the conditioning of the matrix G^0 deteriorated as the ratio $\frac{a}{b}$ decreased. For $\varepsilon \ll 1$ and variation of α we observed similar phenomena to these observed in the case of the disk, namely that there is a minimum in the maximum error for α close to $1/6$.

In the case of $\varepsilon \gg 1$, in order to improve the accuracy of the numerical results, we normalized the fundamental solution by taking

$$\tilde{k}(P, Q) = -\frac{1}{2\pi} \log \frac{r(P, Q)}{R_b} \tag{4.3}$$

instead of the fundamental solution of equation (1.4). As was the case for the disk, we observed that there was a considerable improvement in the accuracy of the solution for large values of R.

ACKNOWLEDGMENT

The authors wish to thank Professor G. Fairweather of the Colorado School of Mines for his useful comments, G. Chimonidis of the University of Cyprus for assistance with the numerical experiments and one of the referees for his/her careful reading of the paper and his/her constructive comments.

REFERENCES

1. Balakrishnan, K., and Ramachandran, P. A. (1999). A particular solution Trefftz method for non-linear Poisson problems in heat and mass transfer. *J. Comput. Phys.* **150**, 239–267.
2. Balakrishnan, K., and Ramachandran, P. A. (2000). The method of fundamental solutions for linear diffusion-reaction equations. *Math. Comput. Modelling* **31**, 221–237.
3. Christiansen, S. (1981). Condition number of matrices derived from two classes of integral equations. *Math. Methods Appl. Sci.* **3**, 364–392.
4. Davis, P. J. (1979). *Circulant Matrices*, John Wiley and Sons, New York.
5. Davis, P. J., and Rabinowitz, P. (1984). *Methods of Numerical Integration*, 2nd ed., Academic Press, Orlando.
6. Fairweather, G., and Karageorghis, A. (1998). The method of fundamental solutions for elliptic boundary value problems. *Adv. Comput. Math.* **9**, 69–95.
7. Freeden, W., and Kersten, H. (1981). A constructive approximation theorem for the oblique derivative problem in potential theory. *Math. Methods Appl. Sci.* **3**, 104–114.
8. Golberg, M. A., and Chen, C. S. (1996). *Discrete Projection Methods for Integral Equations*, Computational Mechanics Publications, Southampton.
9. Gradshteyn, I. S., and Ryzhik, I. M. (1980). *Table of Integrals, Series, and Products*, Academic Press, London.

10. Han, P. S., and Olson, M. D. (1987). An adaptive boundary element method. *Internat. J. Numer. Methods Engrg.* **24**, 1187–1202.
11. Ho-Tai, S., Johnson, R. L., and Mathon, R. (1979). *Software for Solving Boundary-Value Problems for Laplace's Equation Using Fundamental Solutions*, Technical Report 136/79, Department of Computer Science, University of Toronto.
12. Katsurada, M. (1989). A mathematical study of the charge simulation method II. *J. Fac. Sci., Univ. of Tokyo, Sect. 1A, Math.* **36**, 135–162.
13. Katsurada, M. (1990). Asymptotic error analysis of the charge simulation method in a Jordan region with an analytic boundary. *J. Fac. Sci., Univ. of Tokyo, Sect. 1A, Math.* **37**, 635–657.
14. Katsurada, M. (1994). Charge simulation method using exterior mapping functions. *Japan J. Indust. Appl. Math.* **11**, 47–61.
15. Katsurada, M., and Okamoto, H. (1988). A mathematical study of the charge simulation method I. *J. Fac. Sci., Univ. of Tokyo, Sect. 1A, Math.* **35**, 507–518.
16. Katsurada, M., and Okamoto, H. (1996). The collocation points of the fundamental solution method for the potential problem. *Comput. Math. Appl.* **31**, 123–137.
17. Kitagawa, T. (1988). On the numerical stability of the method of fundamental solution applied to the Dirichlet problem. *Japan J. Appl. Math.* **5**, 123–133.
18. Kitagawa, T. (1991). Asymptotic stability of the fundamental solution method. *J. Comput. Appl. Math.* **38**, 263–269.
19. Kupradze, V. D. (1965). *Potential Methods in the Theory of Elasticity, Israel Program for Scientific Translations*, Jerusalem.
20. Kupradze, V. D., and Aleksidze, M. A. (1964). The method of functional equations for the approximate solution of certain boundary value problems. *Comput. Methods Math. Phys.* **4**, 82–126.
21. Mathon, R., and Johnston, R. L. (1977). The approximate solution of elliptic boundary-value problems by fundamental solutions. *SIAM J. Numer. Anal.* **14**, 638–650.
22. *Numerical Algorithms Group Library Mark 16*, NAG(UK) Ltd, Wilkinson House, Jordan Hill Road, Oxford, UK (1993).

Printed In Belgium